Extended X-ray Absorption Fine Structure (EXAFS) Analysis of Disorder and Multiple-Scattering in Complex Crystalline Solids

P. A. O'Day,*,†,‡ J. J. Rehr,§ S. I. Zabinsky,§ and G. E. Brown, Jr.†

Contribution from the Department of Geological and Environmental Sciences, Stanford University, Stanford, California 94305, and Department of Physics, University of Washington, Seattle, Washington 98195

Received September 27, 1993®

Abstract: Quantitative determination of local atomic structure in complex materials using extended X-ray absorption fine structure (EXAFS) analysis was tested on eight inorganic compounds of known structure, including natural and synthetic crystalline solids, at ambient conditions. Our aim was to test the accuracy of experimental and theoretical EXAFS standard functions in determining the number of backscattering atoms (N) at a distance (R) beyond the ligating shell of the central absorber atom where effects from disorder, multiple-scattering, and overlapping shells of atoms may significantly influence the EXAFS spectra. These compounds have complicated structures compared to metals and contain Fe, Co, or Ni as the central absorbing atom and mixtures of second-row (C, O, F), third-row (Si, Cl), and fourth-row (Ca, Fe, Co, Ni) atoms as backscatterers. Comparison of results using both experimental phase-shift and amplitude functions (derived from the EXAFS spectra of the compounds) and those calculated from *ab initio* theory (using the computer code FEFF 5) shows that interatomic distances for single-scattering paths among metal atoms can be determined to within 0.02 Å of values determined independently by X-ray diffraction up to a distance of 4 Å from the central absorber by either method. Theoretical standards calculated using FEFF 5, however, eliminate several drawbacks associated with using experimental standards, such as isolating individual shells of backscattering atoms, obtaining appropriate compounds of high purity and crystallinity, and errors introduced in background subtraction of experimental spectra. Because of the high degree of correlation between N and the Debye–Waller factor (σ^2) in the EXAFS function, the ability to determine N for backscatterers of different Z beyond the first shell is limited by incomplete knowledge of σ^2 for individual absorber–backscatterer paths. For a particular set of backscatterers, N can be determined to better than ±1 if values for σ^2 (±20–30%) can be estimated. For atoms with a small amount of static disorder, estimation methods include using σ^2 values from reference compounds, averaging atomic root-mean-square displacements from X-ray diffraction, or using a correlated Debye model. Static disorder, however, can eliminate completely backscattering amplitudes at ambient temperatures for some absorber–backscatterer pairs and is not necessarily predictable in unknown systems. Multiple-scattering (MS) (for k = 3–12 Å^{-1}) was found to contribute significant amplitude to EXAFS only if focusing occurred among metal atoms. Nonfocused MS, especially for paths involving oxygen atoms, contributed insignificant amplitude to the EXAFS of these compounds for the k-range analyzed.

I. Introduction

Extended X-ray absorption fine structure (EXAFS) spectroscopy has become a popular tool for determination of local atomic structure in a variety of materials. Because it is a nondestructive, atom-specific spectroscopy that can be used for materials in any physical state (solids, liquids, gases), it has been applied to a diverse range of studies, including contaminant uptake, heterogeneous catalysis, structure of biological molecules and semi- and superconducting compounds, optical and electronic properties in solids, and local structure in glasses and amorphous materials.[1] The conclusions drawn in many of these studies rely on quantitative results obtained from the EXAFS analysis of nonmetal compounds with complex crystal structures such as metal oxides, hydroxides, halides, and silicates. As user access to synchrotron X-ray sources increases, more studies using complex inorganic and organic compounds are anticipated. The ability to extract accurate interatomic distances (R), numbers of backscattering atoms (N), and Debye–Waller factors (σ^2) from EXAFS spectra requires comparison with well-known, "standard" phase-shift and amplitude functions, derived from either experimental reference compounds or theoretical calculations. Although several studies have assessed transferability and relative errors for first-coordination-shell absorber–backscatterer pairs,[2] there has been little evaluation of the reliability of higher-shell EXAFS analysis,[3] especially for complex crystalline solids that contain mixtures of low- and high-Z atoms. Furthermore, most studies ignore two factors that may be important in complex materials, variability in atomic static disorder and its effect on σ^2 values, and contributions from multiple-scattering (MS) to EXAFS.

Previously, experimental standards were shown to be more successful than theoretical standards in the accurate determination of R and N, at least in the analysis of atoms ligating the central absorber atom.[2,3] Experimental standards, however, suffer from several limitations, especially for neighboring atoms at distances greater than the first coordination shell from the absorber atom.

* To whom correspondence should be addressed.
† Stanford University.
‡ Present address: Department of Geology & Geophysics, University of California, Berkeley, CA 94720.
§ University of Washington.
® Abstract published in *Advance ACS Abstracts*, March 1, 1994.

(1) See, for example: *Synchrotron Radiation Research*; Winik, H., Doniach, S., Eds.; Plenum Press: New York, 1980. Gurman, S. J. *J. Mater. Sci.* **1981**, *17*, 1541. Brown, G. E., Jr.; Calas, G.; Waychunas, G. A.; Petiau, J. In *Spectroscopic Methods in Mineralogy and Geology*; Hawthorne, F. C., Ed.; Mineralogical Society of America: Washington, DC, 1988; Vol. 18, pp 431–512.

(2) Waychunas, G. A.; Brown, G. E., Jr.; Apted, M. J. *Phys. Chem. Miner.* **1986**, *13*, 31–47. Joyner, R. W.; Martin, K. J.; Meehan, P. J. *Phys. C: Solid State Phys.* **1987**, *20*, 4005–4012. Holmes, D. J.; Batchelor, D. R.; King, D. A. *Surf. Sci.* **1988**, *199*, 476–492.

(3) See recommendations in the following: Lytle, F. W.; Sayers, D. E.; Stern, E. A. *Physica B* **1989**, *158*, 701–722. Report on the international workshops on standards and criteria in XAFS. In *X-ray Absorption Fine Structure*; Hasnain, S. S., Ed.; Ellis Horwood Ltd.: London, 1991; pp 751–770.

0002-7863/94/1516-2938$04.50/0

The most critical of these is the common inability in experimental compounds to isolate EXAFS backscattering from a particular set of atoms from those of other atoms at similar distances. Other difficulties include obtaining pure, well-characterized compounds with appropriate absorber–backscatterer pairs, unknown Debye–Waller factors for different scattering paths, and errors introduced by background subtraction methods in known and unknown experimental spectra. The advent of new *ab initio* theoretical standards such as EXCURVE[4] and FEFF,[5] which are readily available to users in automated computer codes, eliminates many of these drawbacks. Likewise, new theoretical approaches to evaluate contributions from MS to EXAFS spectra, which cannot be predicted with experimental references alone, are beginning to be tested.[6,7]

The increasing application of EXAFS to complex materials and the increasing use of computer-based theoretical standards require evaluation of the analytical approach. Our aim was to examine the ability of experimental standards and the recent *ab initio* theoretical standards in FEFF 5 to determine local atomic structure in a series of known compounds representing a variety of structures and compositions. The approach used here was to analyze the experimental EXAFS of eight well-characterized, crystalline reference compounds, either natural minerals or synthetic inorganic compounds, in which the central absorbing atom is either Fe, Co, or Ni in octahedral coordination and backscattering atoms are C, O, F, Si, Cl, Ca, Fe, Co, and/or Ni. Empirical phase-shift and amplitude functions derived from the experimental spectra, if they could be reasonably isolated for individual sets of backscatterers, were treated alternately as reference and unknown functions. Theoretical phase-shift and amplitude functions for single-scattering and MS paths were calculated on a path-by-path basis with the new MS *ab initio* EXAFS code FEFF 5 (version 5.03[7]). As input to FEFF 5, we used a known atom cluster from each compound and interatomic distances from published X-ray diffraction (XRD) determinations of crystal structure. In this study, we evaluate (1) the reliability of experimental versus *ab initio* phase-shift and amplitude functions in the quantitative analysis of EXAFS for first- and greater-shell atoms and how well backscattering from atoms beyond the first coordination shell can be determined, (2) atomic static disorder and ways in which path-dependent Debye–Waller factors may be constrained; and (3) the importance of MS contributions, which cannot be analyzed using experimental reference functions alone, to observed EXAFS amplitudes beyond the first coordination shell.

II. Methods and Materials

Analysis of EXAFS Spectra. Over the past 20 years, basic EXAFS theory has been well-studied and has developed into a widely-used spectroscopic technique.[8] Atomic information is derived from the normalized absorption fine structure, χ, in terms of structural parameters that relate the phase and amplitude of EXAFS oscillations to the distance, type, and number of backscatterer atoms around the central absorbing atom. The EXAFS function χ is typically plotted in terms of the photoelectron wave vector k, where k is related to kinetic energy of the photoelectron (E) by

$$k = [(2m/\hbar^2)(E - E_0)]^{1/2} \quad (1)$$

E_0 is the threshold energy of the photoelectron at $k = 0$, and m is the mass of the electron. A typical form of the EXAFS function for a single set of atoms (N_R) at a particular distance (R) is given by

$$\chi(k) = \sum_R N_R S_0^2 \frac{|f_{eff}(\pi,k,R)|}{kR^2} \sin(2kR + 2\delta^c + \Phi) e^{-2\sigma^2 k^2} e^{-2R/\lambda} \quad (2)$$

where $f_{eff}(\pi,k,R)$ is the effective curved-wave backscattering amplitude of the scatterer, δ^c and Φ are phase shifts for the absorber and backscatterer, respectively, S_0^2 is a many-body amplitude reduction factor, σ^2 is a Debye–Waller term (or a mean-square relative displacement) assuming a harmonic oscillator, and λ is the mean free path of the electron. Quantitative extraction of R and N_R from experimental data requires that all of the terms affecting $\chi(k)$ must, in some way, be taken into account. This is accomplished by reference to a known structure for which the EXAFS function represented by eq 2 is either measured experimentally or calculated from *ab initio* theory.

Quantitative analysis of EXAFS spectra using experimental standards requires compounds in which the atomic environment of the absorber is similar in the model and the unknown and generally assumes a single-scattering event.[8,9] Normalized, background-subtracted EXAFS for model and unknown spectra are filtered over a similar k-range and Fourier-transformed to produce radial structure functions (RSFs). Peaks in the RSF correspond to pair correlations between the central absorbing atom and local backscattering atoms at a particular distance. In the ideal case, isolation and back Fourier transform of a single peak in the RSF should result in a filtered EXAFS spectrum of frequency and amplitude representative of a single type and number of backscattering atoms at the same distance. The filtered experimental reference spectra are separated into two k-dependent functions, a total phase function that implicitly contains phase shifts for both the absorber ($2\delta^c$) and backscatterer (Φ) atoms and a total amplitude function containing the terms for $f_{eff}(\pi,k,R)$, S_0^2, and λ in eq 2. Nonlinear least-squares methods are used to fit the filtered unknown spectrum to a reference EXAFS spectrum of known R and N by varying R, N_R, and typically, σ^2 in eq 2, and E_0 in Eq 1.

For analysis using *ab initio* standards from FEFF 5, curved-wave phase-shift and amplitude functions were calculated for each compound by specifying a cluster of atoms around the central absorber atom using interatomic distances from XRD. Theoretical values are calculated by FEFF 5 for $2\delta^c$, Φ, $f_{eff}(\pi,k,R)$, a total central atom loss factor (exp[$-Im(2\delta^c)$]), and λ as a function of k for single-scattering or MS paths to the surrounding atoms.[5] Values for S_0^2 and σ^2 in this study were specified: S_0^2 was set at 0.85, a typical value for metals that, in general, appears to be accurate to within about 20%[5]; σ^2 was set equal to 0 in the FEFF 5 calculation of reference spectra so that σ^2 could be treated as an adjustable parameter in fitting unknown spectra. The FEFF 5 code uses a form of eq 2 to calculate $\chi(k)$ for a single path or any combination of single-scattering and MS paths based on the atomic cluster given as input. The $\chi(k)$ function calculated by FEFF 5 for a single-scattering absorber–backscatterer pair was treated in the same way as an experimental reference spectrum in least-squares fitting of unknown spectra. For a few compounds for which Debye temperatures have been reported, we compare σ^2 values determined from a correlated Debye model implemented in FEFF 5[7] to those derived from least-squares fits.

Multiple-scattering calculations in FEFF 5 are based on the fast, accurate scattering-matrix formalism of Rehr and Albers,[10] which is faster, typically, by 1–2 orders of magnitude than exact methods. A key problem in MS analysis is deciding which paths actually contribute to total EXAFS amplitude. In addition to the difficulty of visualizing and enumerating paths, the sheer number of paths grows exponentially with total path length and quickly becomes overwhelming. The importance of a particular path is determined in FEFF 5 by comparing its amplitude, estimated using an approximate plane-wave calculation, to that of the path with the largest amplitude. In almost all cases, the largest amplitude path is the single-scattering path from the nearest atomic neighbor(s) to

(4) Binstead, N.; Campbell, J. W.; Gurman, S. J.; Stephenson, P. C. *S.E.R.C. Daresbury Laboratory EXCURV90 Program*; Daresbury: Warrington, UK, 1990.

(5) Mustre de Leon, J.; Rehr, J. J.; Zabinsky, S. I. *Phys. Rev. B* **1991**, *44*, 4146–4156. Rehr, J. J.; Mustre de Leon, J.; Zabinsky, S. I.; Albers, R. C. *J. Am. Chem. Soc.* **1991**, *113*, 5135–5140.

(6) Frenkel, A. I.; Stern, E. A.; Qian, M.; Newville, M. *Phys. Rev. B* **1993**, *48*, 12449–12458.

(7) Rehr, J. J.; Albers, R. C.; Zabinsky, S. I. *Phys. Rev. Lett.* **1992**, *69*, 3937–3400.

(8) For some reviews, see: Teo, B.-K. *EXAFS: Basic Principles and Data Analysis*; Springer-Verlag: New York, **1986**. Stern, E. A. In *X-ray Absorption: Principles, Applications, Techniques of EXAFS, SEXAFS, and XANES*; Koningsberger, D.C., Prins, R., Eds.; Wiley-Interscience: New York, 1988; pp 3–51. Lytle, F. W. In *Applications of Synchrotron Radiation*; Winick, H., *et al.*, Eds.; Gordon and Breach Science Publ.: New York, 1989; pp 135–223.

(9) Cramer, S. P.; Hodgson, K. O. *Prog. Inorg. Chem.* **1979**, *25*, 1–39. Sayers, D. E.; Bunker, B. A. In *X-ray Absorption: Principles, Applications, Techniques of EXAFS, SEXAFS, and XANES*; Koningsberger, D.C., Prins, R., Eds.; Wiley-Interscience: New York, 1988; pp 211–253.

(10) Rehr, J. J.; Albers, R. C. *Phys. Rev. B* **1990**, *41*, 8139–8149.

Table 1. Names and Structural Formulas of the Reference Compounds Used in this Study[12]

compound[a]	central absorber	structural formula
andradite (n)	Fe	$Ca_3Fe_2Si_3O_{12}$
hedenbergite (n)	Fe	$CaFeSi_2O_6$
cobalt(II) hydroxide (s)	Co	$Co(OH)_2$
cobalt(II) perchlorate hexahydrate (s)	Co	$Co(ClO_4)_2{\cdot}6(H_2O)$
cobalt(II) bis(acetylacetone), dihydrate (s)	Co	$Co(C_5H_7O_2)_2{\cdot}2(H_2O)$
cobalt(II) fluoride (s)	Co	CoF_2
nickel(II) hydroxide (s)	Ni	$Ni(OH)_2$
nepouite (n)	Ni	$Ni_3Si_2O_5(OH)_4$

[a] (n), natural mineral; (s), synthetic compound.

the central atom. The code eliminates negligible paths below a user-set criterion, typically 4% of the mean amplitude of the first-shell backscattering, and thus greatly facilitates calculation and discrimination of a large number of paths. In this study, MS paths were calculated with $\sigma^2 = 0$ in order to overestimate path amplitudes relative to experimental data and identify all paths that may contribute to the EXAFS amplitude.

In least-squares fitting of unknown spectra to experimental or theoretical reference functions, the total number of adjusted parameters should not exceed the number of independent data points (P_i), given by the Nyquist formula,

$$P_i \approx 2\Delta k \Delta R/\pi \tag{3}$$

where Δk and ΔR are the window widths in k- and R-space, respectively, over which the data are Fourier-transformed.[3] When more than one type of backscattering atom, or backscatterers at different distances, are assumed in the fit model, multiple shells of backscattering atoms are required, and thus, it is generally necessary to fix some of the parameters such that P_i is not exceeded. Unfortunately, least-squares fitting of experimental data is complicated by the fact that the adjustable parameters are not necessarily independent. Using eqs 1 and 2, the amplitude of EXAFS oscillations depends on N_R, σ^2, and S_0^2, in addition to $f_{eff}(\pi,k,R)$, and the phase-shift function depends on R, E_0, and, to a smaller extent, σ^2. Implicitly, the formulation of $\chi(k)$ using eq 2 assumes that S_0^2 and σ^2 have the same value for all backscattering atoms (N_R) at the same distance (R), which has been shown to be a reasonable approximation,[11] but not necessarily the same values at different R. Of particular interest in this study is whether some of the variable parameters (e.g., S_0^2, E_0, σ^2) can be fixed at reasonable values for higher-order shells and MS paths, either from the analysis of the first coordination shell or from the analysis of similar classes of reference compounds.

EXAFS Data Collection and Analysis. Well-characterized, crystalline reference compounds were chosen in which the central absorbing metal atom (Me) is either Fe, Co, or Ni and backscattering atoms are C, O, F, Cl, Si, Ca, and/or Me. These compounds are either commercial reagent-grade solids or relatively pure natural minerals whose crystal structures have been determined in previous studies (Table 1).[12] Identity and crystallinity of the samples used for EXAFS analysis were confirmed by powder XRD. For EXAFS data collection, compounds were lightly crushed to powders with an agate mortar and pestle and diluted with enough inert boron nitride to produce about 30% transmission of the incoming beam at the energy of the metal K-absorption edge. Samples were packed carefully into 2-mm-thick aluminum sample holders and sealed with mylar windows, thus ensuring a uniform thickness for all samples.

X-ray absorption spectra were collected on wiggler beamlines IV-1 and IV-3 at the Stanford Synchrotron Radiation Laboratory (SSRL), Stanford, CA, and on bending-magnet beamline X11-A at the National Synchrotron Light Source (NSLS), Brookhaven National Laboratory, NY. Beam current at SSRL varied from 20 to 90 mA at 3 GeV, and the wiggler field was 18 kG. At NSLS, beam current was 100–210 mA at 2.5 GeV. Either Si(111) or Si(220) monochromator crystals were used with an unfocused beam. Higher-order harmonic rejection was achieved by detuning the monochromator such that the maximum transmitted beam flux was reduced by 30–50%. Beam energy was calibrated by assigning the first inflection on the absorption edge of a metal foil to an energy of 7112 eV for Fe, 7709 eV for Co, or 8333 eV for Ni. Spectra were collected in transmission mode using N_2-filled ion chambers at ambient temperature and pressure. For a few of the compounds, spectra were collected in fluorescence mode using a Stern–Heald-type detector.[13] The fluorescence and transmission spectra were compared, and data analysis showed no differences in numerical results, indicating no significant self-absorption in the fluorescence spectra. Multiple scans (2–4) were collected and averaged for each compound to improve the ratio of signal to noise.

The experimental EXAFS spectra were analyzed using the curved-wave formalism[8,9] implemented in the computer code EXAFSPAK, written by G. George (SSRL).[14] Background below the edge jump was subtracted by a linear fit through the pre-edge region and extrapolation through the EXAFS region. Background above the EXAFS region was determined by fitting a cubic spline through three or four data segments. EXAFS spectra were normalized according to the height of the edge step near the absorption edge and extrapolated through the EXAFS region using a Victoreen polynomial and tabulated McMaster coefficients.[15] Normalized EXAFS were converted from energy to k (eq 1) and weighted by k^3. Limits in k- and R-space for forward and back Fourier transforms are listed in Table 2. No windowing function was applied to forward Fourier transforms; a Gaussian window (width = 0.1 Å) was used to filter back Fourier transforms. Nonlinear least-squares curve-fitting (Marquardt algorithm) was used to determine R, N, σ^2, and ΔE_0 (the difference between E_0 for the reference and for the unknown) by fitting reference functions to filtered spectra or, in samples with good signal-to-noise, to normalized EXAFS spectra directly with no Fourier filtering.

In the least-squares analysis of filtered experimental spectra, a relative goodness-of-fit parameter is given in the form of a normalized χ^2 value, ϵ^2, calculated according to

$$\epsilon^2 = (P_i/\nu)(1/N)\sum_{i=1}^{N}(\text{Data}_i - \text{Model}_i)^2 \tag{4}$$

where P_i is the number of independent data points given by eq 3, ν is ($P_i - p$) where p is the number of fit parameters, N is the number of experimental data points, and ($\text{Data}_i - \text{Model}_i$) is the difference between the experimental data and the calculated fit for each point i.[3] Equation 4 neglects division by the standard deviation of individual experimental data points (s_i^2) because there is currently no accepted method for determining these errors, which should include both statistical and nonstatistical errors introduced in data aquisition and in data analysis.[3] Thus, we implicitly assume that s_i^2 is approximately the same for all samples (given that a standard protocol was used for collection and analysis) and report ϵ^2 as a relative measure of the goodness of the least-squares fits among this set of samples. Further details of the procedures used for data reduction are described elsewhere.[16]

III. Results

First Atomic Coordination Shell. The ability of EXAFS analysis to accurately determine R and N for atoms coordinated directly to the absorber atom has been previously demonstrated for reference compounds.[2] Typical errors reported for EXAFS

(11) A recent example is given: Binsted, N.; Strange, R. W.; Hasnain, S. S. *Biochemistry* **1992**, *31*, 12117–12125.

(12) Interatomic distances from X-ray diffraction data quoted throughout are taken from the following sources. Andradite: Novak, G. A.; Gibbs, G. V. *Am. Mineral.* **1971**, *56*, 791–825. Hedenbergite: Cameron, M.; Sueno, S.; Prewitt, C. T.; Papike, J. J. *Am. Mineral.* **1973**, *58*, 594–618. Cobalt(II) hydroxide: Lotmar, W.; Feitknecht, W. *Z. Kristallogr. A* **1936**, *93*, 368–378. Cobalt(II) perchlorate: West, C. D. *Z. Kristallogr.* **1935**, *91*, 480–493. Cobalt-(II) bis(acetylacetone): Bullen, G. J. *Acta Crystallogr.* **1959**, *12*, 703–708. Cobalt(II) fluoride: Baur, W. H. *Acta Crystallogr.* **1958**, *11*, 488–490. Bauer, W. H.; Khan A. A. *Acta Crystallogr. B* **1971**, *27*, 2133–2139. Nickel(II) hydroxide: Lotmar, W.; Feitknecht, W. *Ibid.* Szytula, A.; Murasik, A.; Balanda, M. *Phys. Status Solidi B* **1971**, *43*, 125–128. Nepouite: Zussman, J. G.; Brindley, W.; Comer, J. J. *Am. Mineral.* **1957**, *42*, 133–153. Rucklidge, J. C.; Zussman, J. *Acta Crystallogr.* **1965**, *19*, 381–389.

(13) Lytle, F. W.; Sandstrom, D. R.; Marques, E. C.; Wong, J.; Spiro, C. L.; Huffman, G. P.; Huggins, F. E. *Nucl. Instrum. Methods Phys. Res., Sect. B* **1984**, *226*, 542–548.

(14) Available from Stanford Synchrotron Radiation Laboratory, Stanford, CA.

(15) McMaster, W. H.; Nerr del Grande, N.; Mallett, J. H.; Hubbell, J. H. *Compilation of X-ray Cross Sections*; Report UCRL-50/74, Section 2, Revision 1, Lawrence Radiation Laboratory, University of California, 1969.

(16) O'Day, P. A. Ph.D. Dissertation, Stanford University, 1992 (unpublished). O'Day, P. A.; Parks, G. A.; Brown, G. E., Jr. *Clays Clay Miner.*, in press.

Table 2. Minimum, Maximum, and Width of k for Forward Fourier Transforms and Width of R for Back Fourier Transforms for First (ΔR_1) and Second (ΔR_2) RSF Peaks in the Experimental EXAFS spectra, and the number of independent points (P_i) for the Data Windows Equal to $2\Delta k\Delta R/\pi$

compound	k_{min} (Å^{-1})	k_{max} (Å^{-1})	Δk (Å^{-1})	1st RSF peak		2nd RSF peak	
				ΔR_1 (Å)	P_i	ΔR_2 (Å)	P_i
$Ca_3Fe_2Si_3O_{12}$	3.4	13.2	9.8	1.79	11.2	1.85	11.5
$CaFeSi_2O_6$	3.0	12.8	9.8	1.98	12.4	1.15	7.2
$Co(OH)_2$	3.1	12.7	9.6	1.79	10.9	1.31	8.0
$Co(ClO_4)_2{\cdot}6(H_2O)$	3.0	12.4	9.4	1.77	10.6		
$Co(C_5H_7O_2)_2{\cdot}2(H_2O)$	3.1	12.5	9.4	1.72	10.3		
CoF_2	3.1	12.7	9.6	1.90	11.6	1.30	8.0
$Ni(OH)_2$	3.0	12.7	9.7	1.67	10.4	1.18	7.3
$Ni_3Si_2O_5(OH)_4$	3.1	13.1	10.0	1.60	10.2	1.53	9.7

Table 3. Distance (R), Coordination Number (N), Debye–Waller Factor (σ^2), and Difference in Threshold Energy (ΔE_0) between Reference and Unknown from Nonlinear Least-Squares Fits of Filtered First-Shell EXAFS Spectra[a]

compound	Me–L (expt reference)[b]					Me–L (FEFF reference)[c]					Me–L (XRD)	
	R (Å)	N	σ^2 (Å^2)	ΔE_0 (eV)	ϵ^2	R (Å)	N	σ^2 (Å^2)	ΔE_0 (eV)	ϵ^2	R (Å)	N
$Ca_3Fe_2Si_3O_{12}$	2.00_2	4.9	0.0010	3.7	0.59	2.00_6	4.5	0.0030	−0.9	0.38	2.024	6
$CaFeSi_2O_6$	2.10_3	4.7	0.0047	−0.5	0.10	2.10_0	4.4	0.0058	−5.9	0.34	2.087	2
											2.140	2
											2.164	2
$Co(OH)_2$						2.09_7	6.0	0.0067	5.9	0.38	2.097	6
$Co(ClO_4)_2{\cdot}6(H_2O)$	2.07_5	7.8	0.0054	−2.6	0.27	2.06_9	7.6	0.0079	0.6	0.28	2.125	6
$Co(C_5H_7O_2)_2{\cdot}2(H_2O)$	2.02_6	3.5	0.0023	−4.0[d]	0.50	2.03_6	3.5	0.0052	−2.0[d]	0.64	2.039	2
											2.045	2
											2.215	2
CoF_2	2.05_3	8.4	0.0037	−2.1	0.91	2.03_2	6.0	0.0053	−5.1	0.51	2.027	2
											2.049	4
$Ni(OH)_2$[e]	2.06_1	6.0	0.0043	−4.8	0.69	2.06_1	5.6	0.0061	2.0	0.47	2.05–2.12	6
$Ni_3Si_2O_5(OH)_4$[e]	2.03_6	7.2	0.0043	−6.5	0.59	2.03_1	6.3	0.0060	−9.6	0.28	2.03(?)	3
											2.08(?)	3

[a] The goodness-of-fit parameter (ϵ^2) is given by eq 4. EXAFS results are compared to interatomic distances reported from XRD data (from references in Table 1). For all compounds, only one shell of ligating atoms could be refined significantly in the least-squares fit, although XRD indicates minor distortion of the coordinating octahedra in some of the compounds. [b] Me = Fe, Co, or Ni; L = O for all compounds except CoF_2 where L = F. Reference experimental phase-shift and amplitude functions are from $Co(OH)_2$ for six O atoms at 2.097 Å. [c] Reference FEFF theoretical phase-shift and amplitude functions are for Me–L R and N calculated using atomic positions from XRD. [d] Fixed parameter. [e] Disagreement in Ni–O distances reported from XRD and EXAFS data for this compound. See Table 6.

analysis of first-shell atoms are $R \leq 0.02$ Å and $N \leq 20\%$ for low values of σ^2, although the number of adjustable parameters in the least-squares fit is not always reported. Fits to filtered first RSF peaks are compared in Table 3 using (1) experimental phase-shift and amplitude functions for Co–O from $Co(OH)_2$ as the reference for all other compounds and (2) theoretical functions from FEFF for Me–L (where Me is the central metal atom absorber and L is the coordinating ligand, either six O or six F) using the known crystal structure of each compound to generate the FEFF theoretical functions. Four parameters were varied in the analysis of each compound: R, N, σ^2, and E_0. In all of these compounds, the central metal atom is octahedrally coordinated by O or F, and little difference was found using an experimental model ($Co(OH)_2$) with $Z \pm 1$ from the unknown. The average difference in the Me–L distance determined using the experimental model versus the FEFF model was 0.007_7 Å (SD = 0.006_6); the maximum difference found for R was for CoF_2 ($\Delta R = 0.021$ Å). Distances determined by EXAFS were in good agreement with values reported from XRD data (Table 3). In compounds in which the coordinating octahedron is distorted slightly, the distortion was generally not great enough such that two or more sets of first-shell distances could be refined in the least-squares fit without constraining some of the fit parameters.

Previous studies have noted the difficulty in obtaining coordination numbers (N) with an accuracy of better than about 20%. Coordination numbers are derived from the EXAFS amplitude function, which can be affected by a number of different factors, including differences in background subtraction, variations in the magnitudes of σ^2 and S_0^2, and windowing of RSF peaks. Comparison of N determined by experimental and FEFF models (Table 3) shows that the FEFF determinations of N were better than the experimental reference in more cases, probably because of differences in experimental background absorption in the reference and unknown spectra (the fit for $Co(C_5H_7O_2)_2{\cdot}2(H_2O)$ is discussed in the next section). Both N and σ^2, which are highly correlated, were varied simultaneously in the least-squares analysis. Table 3 shows that N is within 20% of the known value using the experimental reference only when the atomic structures are very similar and there is no distortion in the coordinating octahedron; for example, compare $Co(OH)_2$ and $Ni(OH)_2$. Coordination numbers for both of the Fe-absorber compounds (andradite ($Ca_3Fe_2Si_4O_{12}$) and hedenbergite ($CaFeSi_2O_6$)) were systematically low (by 22–27%) using either the experimental or FEFF references. This suggests that some amplitude reduction may be related to multielectron processes, associated primarily with the central absorber atom, that are accounted for by the S_0^2 term in eq 2.[17] The error in N can be reduced if a value for S_0^2 is estimated from reference compounds with similar central-absorber coordination. For example, first-shell cross fits between andradite and hedenbergite show that $S_0^2 = 0.75$–0.80 (rather than $=0.85$ used in the FEFF calculation) gives a refined N within 5% of the known value.

In order to obtain accurate distances from least-squares fits, it is essential to let E_0 be an adjustable parameter, and the ΔE_0 values determined from experimental and theoretical references should be different. Depending on whether the reference functions are experimental or theoretical, variation in E_0 of a few electronvolts accounts for different factors, e.g., chemical shifts, ionicity, and calibration errors. In the experimental case, ΔE_0 is the difference in E_0 between the experimental reference and the unknown spectra, which may be up to several electronvolts for different compounds and experimental conditions even when

(17) Stern, E. A.; Bunker, B.; Heald, S. M. In *EXAFS Spectroscopy*; Teo, B.-K., Joy, D. C., Eds.; Plenum Press: New York, 1981; pp 59–80.

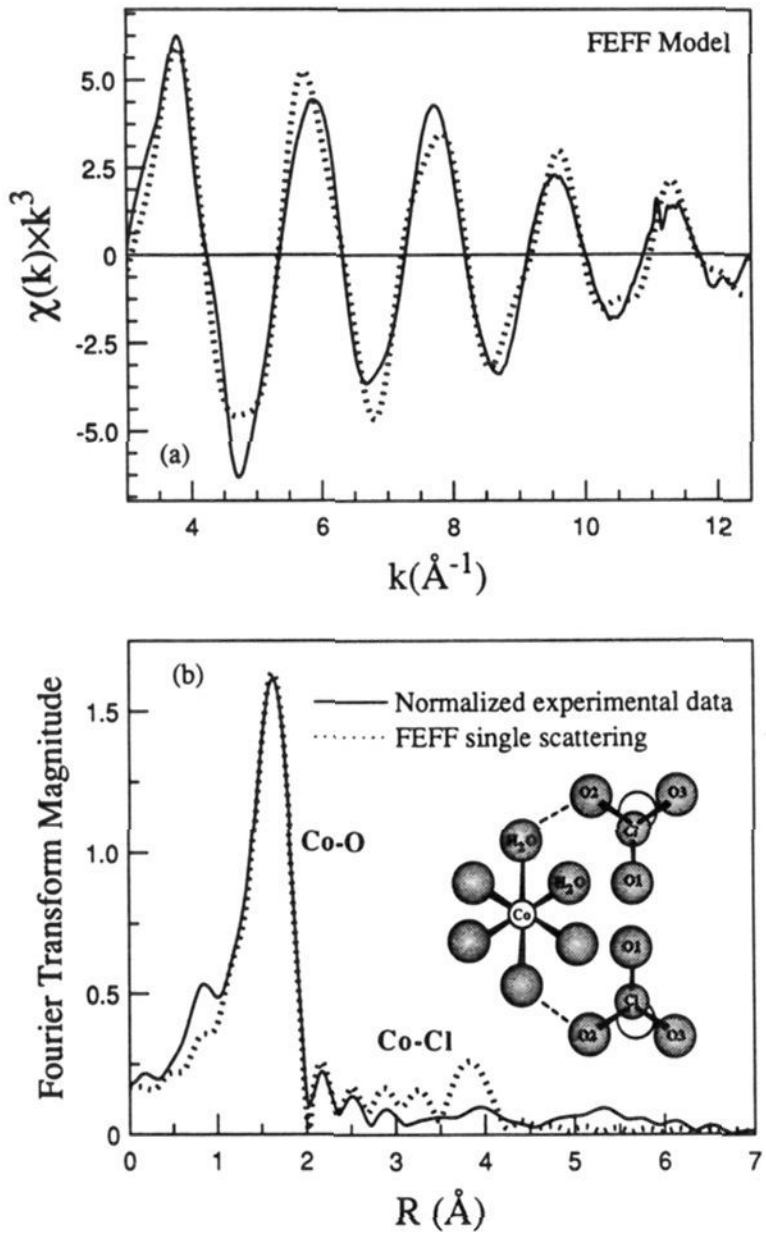

Figure 1. (a) Normalized, experimental EXAFS spectrum (solid line) and FEFF theoretical model (dots) of $Co(ClO_4)_2 \cdot 6(H_2O)$ (Co(per)). The FEFF spectrum is composed of all single-scattering paths out to 4.35 Å from Co using the same value for σ^2 (=0.0077 Å^2). (b) Forward Fourier transforms (uncorrected for phase shift) of experimental data and FEFF model shown in a. Note that the FEFF model predicts a peak in the RSF from O and Cl atoms at 4.05–4.09 Å that is not present in the experimental data.

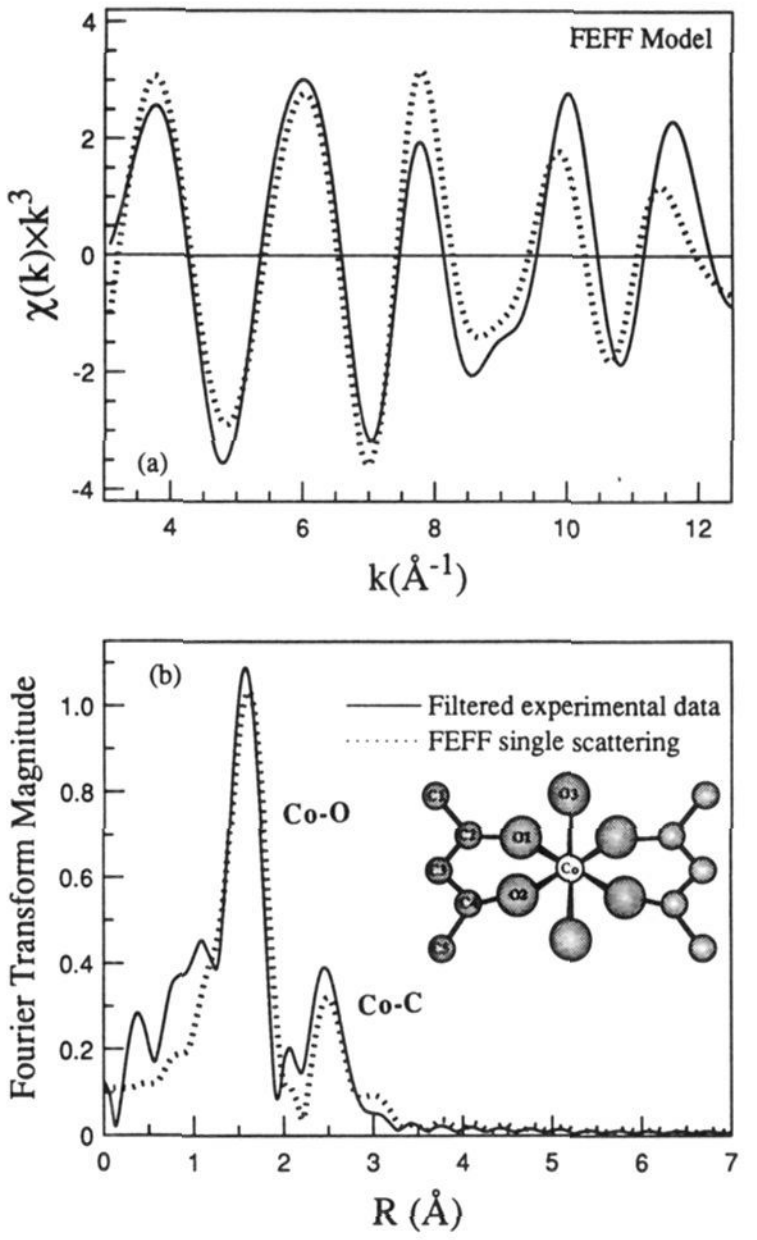

Figure 2. Filtered, experimental EXAFS spectrum of $Co(C_5H_7O_2)_2 \cdot 2(H_2O)$ (Co(acac)) (solid line) and nonlinear least-squares fit (dots) using FEFF theoretical phase-shift and amplitude functions as the reference: (a) fit assuming four O at 2.04 Å, four C at 2.94 Å, two C at 3.26 Å; σ^2 treated as an adjustable parameter for each shell; (b) RSFs (uncorrected for phase shift) of experimental data and least-squares fit shown in a.

a consistent method of calibration is used. In the theoretical case, ΔE_0 is the difference between the E_0 value calculated in the FEFF 5 model, which is estimated by the chemical potential of a homogeneous electron gas at the average interstitial charge density,[5] and the E_0 value chosen (arbitrarily) for the experimental unknown. Variation in E_0 depends primarily on the central absorber atom and the isotropy of the electronic potential in the compound. Thus, for relatively homogeneous compounds, we have found that E_0 values determined from first-shell fits can be fixed reliably in fits to higher-shell backscatterers if the same experimental or theoretical model is used, thereby reducing one adjustable parameter. A sensitivity analysis of our reference compounds shows that a shift in ΔE_0 of at least 3–4 eV is needed to produce a shift in R that is greater than a typical experimental error of ±0.02 Å.

Single-Scattering beyond the First Coordination Shell. The reliability of structural information from EXAFS analysis for atomic neighbors beyond the ligating shell of a central atom has not been investigated as extensively as for first-shell atoms. One of the most difficult and common problems in such analyses is the presence of more than one type of atom at a similar distance. A least-squares analysis requires fitting multiple shells of atoms and, thus, can result in a large number of adjustable, highly correlated parameters. This is especially common in silicate and oxide minerals, which often contain mixtures of atoms of different Z. In addition, values of σ^2 for different absorber–backscatterer pairs are often not known and are not transferable from first-shell fits. In many cases, it is difficult to obtain experimental reference compounds in which the RSF peak of a single absorber–backscatterer pair of appropriate type and distance can be isolated from other overlapping atoms. Consequently, it is important to evaluate the ability of theoretical calculations to generate reliable phase-shift and amplitude functions for backscattering atoms beyond the first shell. Three different cases are discussed below for the analysis of atoms beyond the first coordination shell using experimental data and *ab initio* functions generated by FEFF 5.

A. Contributions from Low-Z Backscattering Atoms. An often-used simplification in EXAFS analysis is to ignore contributions from low-Z elements (usually $Z < 10$) beyond the first coordination shell and to assume that backscattering is dominated by higher Z atoms. This assumption was tested in two of the reference compounds (Table 1), cobalt(II) perchlorate hexahydrate ($Co(ClO_4)_2 \cdot 6(H_2O)$) and cobalt(II) bis(acetylacetone) dihydrate ($Co(C_5H_7O_2)_2 \cdot 2(H_2O)$) (referred to as Co(per) and Co(acac), respectively). In both of these compounds, the central absorber (Co) is coordinated directly by six O atoms.

In Co(per), the O ligands are six H_2O molecules bridged by perchlorate molecules. Thus, there are six O atoms at 2.125–2.126 Å, and the next-nearest backscattering atoms are six O at 4.050–4.060 Å and one Cl at 4.089 Å (using atomic positions from XRD[12]). The first-shell atomic arrangement is reflected in the experimental RSF (Figure 1), which contains a prominent first peak due to the six O atoms but no significant peaks at higher R. A theoretical EXAFS spectrum was generated by FEFF using atomic positions for Co(per) from XRD and composed of all single-scattering paths out to 4.35 Å from Co (MS paths

Table 4. Distance (R), Number of Backscatterers (N), Debye–Waller Factor (σ^2), and Difference in Threshold Energy (ΔE_0) between Reference and Unknown from Nonlinear Least-Squares Fits of Filtered Second-Shell EXAFS Spectra[a]

		Me–Me (expt reference)					Me–Me (FEFF reference)					Me–Me (XRD)		
		Me–Me	R (Å)	N	σ^2 (Å^2)	ΔE_0[b] (eV)	ϵ^2	R (Å)	N	σ^2 (Å^2)	ΔE_0[b] (eV)	ϵ^2	R (Å)	N
$Co(OH)_2$[c]		Co–Co	3.16_5	6.9	0.0010	3.7	0.13	3.17_3	6.7	0.0066	6.3	0.40	3.173	6
$Ni(OH)_2$[d]		Ni–Ni	3.12_0	5.0	0.0030	−4.8	0.21	3.12_5	6.2	0.0068	2.0	0.36	3.09–3.12	6
CoF_2[d]	fit I	Co–Co	3.16_1	2.0[e]	0.0011	−2.1	0.35	3.16_3	2.0[e]	0.0037	4.0	0.83	3.177	2
			3.68_0	8.0[e]	0.0057	−2.1		3.68_3	8.0[e]	0.0069	4.0		3.681	8
	fit II		3.16_2	3.0	0.0040[e]	−2.1	0.52	3.16_5	2.6	0.0055[e]	4.0	1.18		
		3.68_2	7.3	0.0040[e]	−2.1		3.68_4	6.9	0.0055[e]	4.0				

[a] A relative goodness-of-fit parameter (ϵ^2) is given by eq 4. EXAFS results using experimental reference functions or *ab initio* functions calculated by FEFF 5 are compared to interatomic distances reported from XRD data (from references in Table 1). [b] In all fits, ΔE_0 was determined in least-squares fits to the filtered EXAFS of the first RSF peak and fixed in the fits shown here. [c] Experimental reference functions: Ni–Ni from $Ni(OH)_2$. [d] Experimental reference functions: Co–Co from $Co(OH)_2$. [e] Fixed parameter.

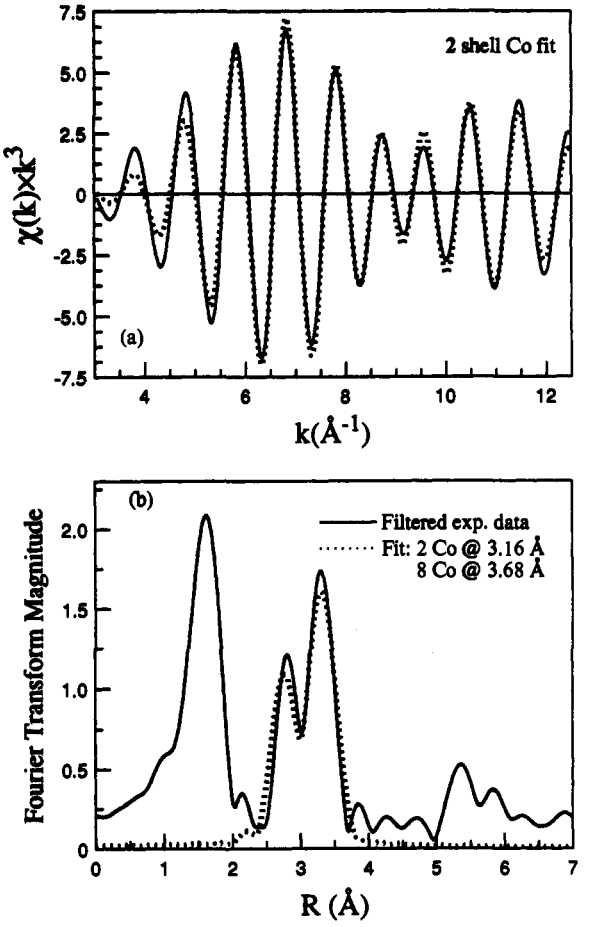

Figure 3. Filtered, experimental EXAFS spectrum (solid line) of the second RSF peak of CoF_2 and nonlinear least-squares fit (dots) using empirical phase-shift and amplitude functions of Co–Co from $Co(OH)_2$ as the reference: (a) best fit assuming two shells of Co atoms with R and σ^2 treated as adjustable parameters and N and ΔE_0 fixed for each shell (see Table 4); (b) RSFs (uncorrected for phase shift) of experimental data and least-squares fit shown in a.

were determined by FEFF to be insignificant). The filtered experimental EXAFS of the first RSF peak was fit to FEFF phase-shift and amplitude functions for six O at 2.125 Å to determine values for σ^2 (0.0077 Å^2) and ΔE_0 (0.2 eV) (R and N fixed). These values were then used for all paths in the theoretical model and compared to the experimental data. The FEFF theoretical model (Figure 1) predicts a peak in the RSF from O and Cl atoms at 4.05–4.09 Å that is not present in the experimental spectrum (using $\sigma^2 = 0.0077$ Å^2). This comparison, in agreement with previous studies, suggests a reduction in backscattering amplitudes from high values of σ^2 for more distant, low-Z atoms (especially at room temperature) and indicates that first-shell σ^2 values are not transferable to more distant atoms of the same Z.

A similar comparison between theory and experiment was made using a FEFF model for Co(acac). In this structure, four of the six coordinating O atoms around Co are attached to four C atoms of the acetylacetone (acac) chelate group, resulting in a tetragonally distorted octahedron around Co. The interatomic distances around Co from XRD data[12] are two O at 2.039 Å, two O at 2.045 Å, two O at 2.215 Å, two C at 2.935 Å, two C at 2.952 Å, and two C at 3.264 Å. Best fits either to the filtered EXAFS of first and second RSF peaks separately or to the entire normalized, unfiltered EXAFS spectrum indicate no significant backscattering from the two axial O atoms at 2.215 Å (Figure 2). This was the case whether one or two shells of O atoms (four O at 2.04, two O at 2.215 Å) were assumed in the fit model (i.e., a two-shell fit always converged to one shell of approximately four O atoms at 2.04 Å). The second RSF peak is apparently from C backscattering only. It is not obvious why there is no backscattering amplitude from the axial oxygen atoms, but perhaps there is large static disorder for these atoms. A theoretical FEFF EXAFS spectrum composed of one shell of O atoms (four O at 2.042 Å) and two shells of C atoms (four C at 2.944 Å and two C at 3.264 Å) was fit to the experimental spectrum with N and R fixed and σ^2 treated as an adjustable parameter (three variables). As shown in Figure 2, the theoretical spectrum reproduces the major features in the experimental spectrum, although it does not produce a perfect fit, probably in part because of difficulties in background subtraction for this particular experimental spectrum. In Co(acac), backscattering from C atoms beyond the ligating shell at 2.944 and 3.264 Å contributes significantly to the EXAFS.

These two examples show that, at ambient temperatures, (1) backscattering from O is probably not significant in most compounds at distances greater than ≈3.5–4 Å and (2) in the absence of higher Z backscatterers, low-Z elements such as C beyond the ligating shell (at <3.5 Å) can contribute to EXAFS in some compounds; however, unpredictable disorder effects can reduce backscattering amplitudes below background even for oxygen atoms bonded to the central absorber.

B. Evaluation of Metal–Metal Correlations. Metal–metal (Me–Me) contributions to EXAFS for metal atoms not directly bonded to the central absorber were analyzed in three compounds, $Co(OH)_2$, $Ni(OH)_2$, and CoF_2, using both experimental and theoretical reference functions. In this group of compounds, backscattering is dominated by Me atoms in high-symmetry sites with low degrees of static disorder, and the only other backscattering atoms are of much lower Z (O or F). Cross-comparison between $Co(OH)_2$ and $Ni(OH)_2$, which have identical crystal structures, produced excellent fit results compared with values from XRD (the maximum deviation in R was ±0.008 Å, and in N, ±17%) when R, N, and σ^2 were varied simultaneously (Table 4). Similar results were obtained using either experimental or theoretical (FEFF) reference functions. The good agreement in

Table 5. Distance (R), Number of Backscatterers (N), Debye–Waller Factor (σ^2), and Difference in Threshold Energy (ΔE_0) between Reference and Unknown from Nonlinear Least-Squares Fits of Filtered Second-Shell EXAFS Spectra[a]

				Me–B (EXAFS)					Me–B (XRD)			
compound		Me	B	R (Å)	N	σ^2 (Å^2)	ΔE_0[b] (eV)	ϵ^2	R (Å)	N	σ^2[c] (Å^2)	Debye σ^2[d] (Å^2)
$Ca_3Fe_2Si_3O_{12}$ (andradite)		Fe	Si	3.37[e]	6.0[e]	0.0048	−0.9	0.43	3.370	6	0.0061	0.0041
			Ca	3.37[e]	6.0[e]	0.0069	−0.9		3.370	6	0.0057–0.0068	0.0033
$CaFeSi_2O_6$ (hedenbergite)		Fe	Fe	3.10_1	1.9	0.0060[e]	−5.9	0.14	3.109	2	0.0049–0.0061	0.0033
			Ca			>0.015	−5.9		3.224	2	0.0056–0.0086	0.0040
			Si	3.31_2	3.8	0.0048[e]	−5.9		3.297	4	0.0046–0.0057	0.0050
			Si			>0.015	−5.9		3.516	2	0.0046–0.0057	0.0050
$Ni_3Si_2O_5(OH)_4$[f] (nepouite)	fit I	Ni	Ni	3.05_7	7.1	0.0030[e]	−6.5	1.14	3.05–3.07	6		0.0042
			Si	3.28_8	3.2	0.0048[e]	−1.5		3.20–3.26	2		0.0071
	fit II	Ni	Ni	3.05_4	6.0[e]	0.0021	−6.5	1.14	3.05–3.07	6		0.0042
			Si	3.29_6	2.0[e]	0.0010	−1.5		3.20–3.26	2		0.0071

[a] A relative goodness-of-fit parameter (ϵ^2) is given by eq 4. Theoretical phase-shift and amplitude functions from FEFF 5 were used for Fe–Si, Fe–Ca, Fe–Ca, Fe–Fe, and Ni–Si fits; experimental phase-shift and amplitude functions for Co–Co from $Co(OH)_2$ were used for the Ni–Ni fit. EXAFS results are compared to interatomic distances reported from XRD data.[12] Isotropic and anisotropic atomic root-mean-square displacements from XRD were used to estimate minimum and maximum values of σ^2 for individual absorber–backscatterer pairs. Debye σ^2 was calculated using a correlated Debye model[18,20] implemented in FEFF 5. [b] In all fits, ΔE_0 was determined in least-squares fits to the filtered EXAFS of the first RSF peak and fixed in the fits shown here. [c] Calculated by averaging XRD atomic root-mean-square displacements given by Novak and Gibbs (1971) for andradite and Cameron *et al.* (1973) for hedenbergite.[12] [d] Calculated using the following Debye temperatures given by Kieffer:[21] 738 K for andradite; 654 K for hedenbergite (value for diopside, $CaMgSi_2O_6$, Mg–Fe solid-solution end-member); 525 K for nepouite (value for talc, $Mg_6Si_8O_{20}(OH)_4$). [e] Fixed parameter. [f] Disagreement in Ni–B distances reported from XRD and EXAFS data for this compound. See Table 6.

distances for second-neighbor atoms demonstrates the validity of fixing ΔE_0 at the value derived from fitting first-shell atoms.

Analysis of second-neighbor Me–Me EXAFS in CoF_2 is complicated by the presence of different numbers of Co atoms at two different, partially overlapping distances (two Co at 3.177 Å; eight Co at 3.681 Å), giving rise to a split second peak in the RSF (Figure 3). We examined the consequences of constraining different adjustable parameters in fits to the filtered EXAFS spectrum back-transformed over the entire second peak (R = 2.5–3.7 Å) and assuming two shells of Co atoms. Because of the high degree of correlation between N and σ^2, N was fixed and σ^2 adjusted in fit I, and N was adjusted and σ^2 fixed in fit II. The maximum difference in R between the EXAFS and XRD determinations is 0.016 Å for both Co–Co distances regardless of whether N or σ^2 was fixed in the fit (Table 4). When N was fixed, refinement of σ^2 produced different values for each shell for either experimental or theoretical reference functions (Table 4). When σ^2 was fixed at the same value for each shell (0.0040 or 0.0055 Å^2), the refined values of N were underestimated for the eight backscattering Co atoms (N = 7.3 (experimental) or 6.9 (FEFF)) and overestimated for the two at a closer distance (N = 3.0 (experimental) or 2.6 (FEFF)). The amount of variability in the refined values of σ^2 for N fixed or varied suggests uncertainties in σ^2 of about 20–30%. As shown in previous work,[9,18] it cannot be assumed that the same absorber–backscatterer pair at different distances necessarily has the same σ^2 value. Backscattering is path-dependent for absorber–backscatterer pairs that are not bonded directly to each other, and reduction in amplitude may occur from static and thermal disorder and from electronic factors that are poorly understood.[18] This analysis points out a typical problem, discussed further in the next section, of determining accurately R, N, and σ^2 for overlapping shells of atoms.

C. Mixed-Z Shells and Debye–Waller Factors. In many compounds, a typical problem in EXAFS analysis is the "deconvolution" of backscattering contributions from two or more atoms of different Z at overlapping distances. This type of analysis is especially difficult when one set of atoms is heavier, and therefore a much stronger backscatterer, than the others. Because of the large number of possible adjustable parameters when multiple shells are assumed in a fit, in general, some parameters must be fixed. As shown above, ΔE_0 can be determined with reasonable accuracy by analysis of the first shell and fixed in subsequent fits of higher-order shells in the same reference-unknown system. In this section, we examine transferability of σ^2 from reference compounds with absorber–backscatterer pairs similar to the unknown system. In addition, we discuss the use of atomic displacements determined from XRD and the applicability of a correlated Debye model in constraining values of σ^2 for individual absorber–backscatterer pairs. We first consider only single-scattering paths; analysis of MS with FEFF 5 (discussed in the next section) shows that MS does not contribute to second-neighbor EXAFS amplitudes in these compounds.

Single-scattering from second-neighbor atoms was examined in three silicate compounds:[12] andradite ($Ca_3Fe_2Si_3O_{12}$, Me = Fe), hedenbergite ($CaFeSi_2O_6$, Me = Fe), and nepouite ($Ni_3Si_2O_5(OH)_4$, Me = Ni). In these three compounds, Si atoms overlap with Ca and/or second-neighbor Me atoms at the distances shown in Table 5. Atomic positions are well-known from XRD data for andradite and hedenbergite (Table 5). Atomic positions have not been reported for nepouite, but they are known for lizardite, the Mg end-member of a Mg–Ni solid solution of this mineral. The nepouite used in this study has been studied previously by EXAFS, and there is some disagreement in the reported R values from XRD and EXAFS (summarized in Table 6).[19]

Transferability of σ^2 values for Fe–Si and Fe–Ca correlations was assessed by fitting FEFF reference functions to the filtered, experimental spectrum of andradite in which R, N, and ΔE_0 were fixed and σ^2 was varied for each atomic shell constituting the second RSF peak. The experimental EXAFS spectrum of hedenbergite was then used as an unknown to examine single-scattering contributions from four different types of second-neighbor atoms at distances spanned by the second RSF peak (Table 5). The filtered EXAFS spectrum was fit to FEFF functions for each of four atomic shells, and all parameters were fixed on known values except σ^2 for each shell (four parameters varied). The best fit produced large values of σ^2 (>0.015 Å^2) for Fe–Ca at 3.224 Å and Fe–Si at 3.516 Å such that these shells

(18) Crozier, E. D.; Rehr, J. J.; Ingalls, R. In *X-ray Absorption: Principles, Applications, Techniques of EXAFS, SEXAFS, and XANES*; Koningsberger, D. C., Prins, R., Eds.; Wiley-Interscience: New York, 1988; pp 373–442.

(19) Interatomic distances for $Ni(OH)_2$ and $Ni_3Si_2O_5(OH)_4$ are taken from the following sources in addition to those given in ref 12: Oswald, H. R.; Asper, R. In *Preparation and Crystal Growth of Materials with Layered Structures*; Lieth, R. M. A., Ed.; Reidel Publ.: Dordrecht, Netherlands, 1977; pp 77–140. Manceau, A.; Calas, G. *Am. Mineral.* **1985**, *70*, 549–558. Manceau, A.; Calas, G. *Clay Miner.* **1986**, *21*, 341–360. Bonneviot, L.; Clause, O.; Che, M.; Manceau, A.; Decarreau, A.; Villain, F.; Bazin, D.; Dexpert, H. *Physica B* **1989**, *158*, 43–44. Bonneviot, L.; Clause, O.; Che, M.; Manceau, A.; Dexpert, H. *Catal. Today* **1989**, *6*, 39–46.

Table 6. Values Reported in the Literature for Interatomic Distances in $Ni(OH)_2$ and $Ni_3Si_2O_5(OH)_4$ (Nepouite) by Different Experimental Methods[12,19]

compound	R_{Ni-O} (Å)	R_{Ni-Ni} (Å)	R_{Ni-Si} (Å)	method[a]	reference
$Ni(OH)_2$	2.111	3.117		XRD	Lotmar and Feitknecht (1936)
	2.07	3.12		XRD	Oswald and Asper (1977)
	2.121	3.130		ND	Szytula *et al.* (1971)
	2.05	3.09		EXAFS	Manceau and Calas (1986)
$Ni_3Si_2O_5(OH)_4$ (nepouite)	2.03, 2.08	3.07	3.26	XRD[b]	Zussman *et al.* (1957); Rucklidge and Zussman (1965)
	2.03	3.06	3.20	EXAFS	Manceau and Calas (1986)
	2.08	3.06	*c*	EXAFS	Manceau and Calas (1985)
	c	3.05	*c*	EXAFS	Bonneviot *et al.* (1989, *Physica B*; 1989, *Catal. Today*)

[a] XRD, X-ray diffraction; ND, neutron diffraction; EXAFS, extended X-ray absorption fine structure. [b] Mg–O, Mg–Mg, and Mg–Si distances from refinement of the lizardite structure ($Mg_3Si_2O_5(OH)_4$), isostructural with $Ni_3Si_2O_5(OH)_4$. [c] Not reported.

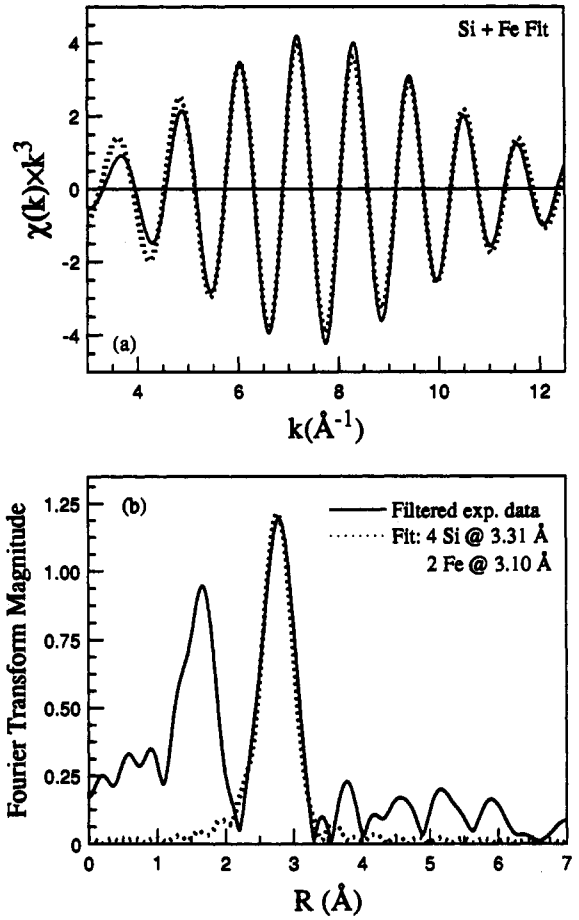

Figure 4. Filtered, experimental EXAFS spectrum (solid line) of the second RSF peak of hedenbergite and nonlinear least-squares fit (dots) using FEFF theoretical phase-shift and amplitude functions as the reference: (a) best fit assuming one shell of Si atoms and one shell of Fe atoms; (b) RSFs (uncorrected for phase shift) of experimental data and least-squares fit shown in a.

contributed no amplitude to the EXAFS. These large refined values for σ^2 are probably due to high static disorder for Ca (discussed below), too few Si atoms (N = 2) at 3.516 Å to distinguish from O atoms at similar distances, and high correlation among the fitted σ^2 values. The filtered spectrum for hedenbergite can be reasonably fit by assuming only two shells: Fe–Fe at 3.109 Å and Fe–Si at 3.297 Å. In this fit model, N could be refined by fixing σ^2 on values determined from andradite for Fe–Si, and from $Co(OH)_2$ and CoF_2 (Co–Co) for Fe–Fe, and by varying R and N for each shell (Figure 4 and Table 5). This fit produced excellent agreement of R and N with values from XRD (ΔR = 0.008 Å and ΔN = 0.1 for Fe–Fe; ΔR = 0.015 Å and ΔN = 0.2 for Fe–Si).

Ambient temperature XRD studies of andradite and hedenbergite[12] suggest that a high degree of atomic static disorder for large cations such as Ca is at least partly responsible for their low EXAFS backscattering amplitudes. Minimum and maximum values of σ^2 for absorber–backscatterer pairs were estimated by averaging the isotropic and anisotropic atomic root-mean-square (rms) displacements for individual atoms from XRD refinements (Table 5). The ambient temperature XRD results showed slightly higher mean anisotropic rms displacements for Ca than for tightly-bound cations such as Si. Estimates of σ^2 for Si and Fe from XRD rms displacements fall into the range derived from EXAFS fits (Table 5) and suggest that XRD data for reference compounds may be useful in estimating EXAFS σ^2 in unknowns with similar atoms and low static disorder. For atoms with high, anisotropic displacements like Ca, however, XRD data were found to underestimate significantly the EXAFS σ^2 value at room temperature. In hedenbergite, for example, fits to the EXAFS data suggest a value of $\sigma^2 > 0.015$ Å^2 for Fe–Ca, such that there is no significant backscattering from Ca, rather than $\sigma^2 = 0.0056$–0.0086 Å^2 calculated from the XRD rms displacements. Quantitative analysis of second-shell EXAFS could probably be improved by collecting data at low temperatures to reduce thermal disorder or over a range of temperature to estimate the thermal σ^2 contribution. Constraining σ^2 from XRD and temperature-dependent studies may allow better refinement of R and N in complicated compounds where overlapping shells are difficult to analyze.

In another test, the filtered EXAFS of nepouite was fit using Co–Co reference functions from $Co(OH)_2$ by assuming, initially, backscattering only from Ni atoms at a single distance. A best fit obtained by varying R, N, and σ^2 matches the experimental EXAFS phase in the middle part of the k-range, but there is a phase mismatch at high and low k and a mismatch in the peak position in the RSF that suggests the presence of another backscatterer (Figure 5a,b). An improved fit was produced by assuming Ni and Si as backscattering atoms, fixing σ^2 at values determined from andradite (Me–Si) and $Co(OH)_2$ (Me–Me), and varying R and N for each atomic shell (Figure 5c,d). Values of R and N from this fit (fit I) are in good agreement with those reported by previous EXAFS and XRD analysis (Tables 5 and 6). Both Ni and Si atoms in nepouite were found to contribute to the EXAFS in this compound, although backscattering is dominated by Ni. Fixing N and refining σ^2 (fit II, Table 5) suggests that σ^2 values may be slightly lower in this compound than those assumed from andradite and $Co(OH)_2$ in fit I or, alternatively, that the reference value of S_0^2 should be slightly higher.

Because of the high degree of correlation between N and σ^2, it is desirable to be able to independently estimate σ^2 in systems in which N is unknown and no information about σ^2 is available from XRD (e.g., for glasses or amorphous solids) or other methods. Values of σ^2 calculated using a correlated Debye model[18,20] have been applied with success in the EXAFS analysis of compositionally-simple, high-symmetry compounds such as alkali halides[6] and metals.[7] Using the Debye model (implemented in FEFF 5), we calculated absorber–backscatterer σ^2 values at 298 K for

(20) Beni, G.; Platzman, P. M. *Phys. Rev. B* **1976**, *14*, 1514–1518. Sevillano, E.; Meuth, H.; Rehr, J. J. *Phys. Rev. B* **1979**, *20*, 4908–4911.

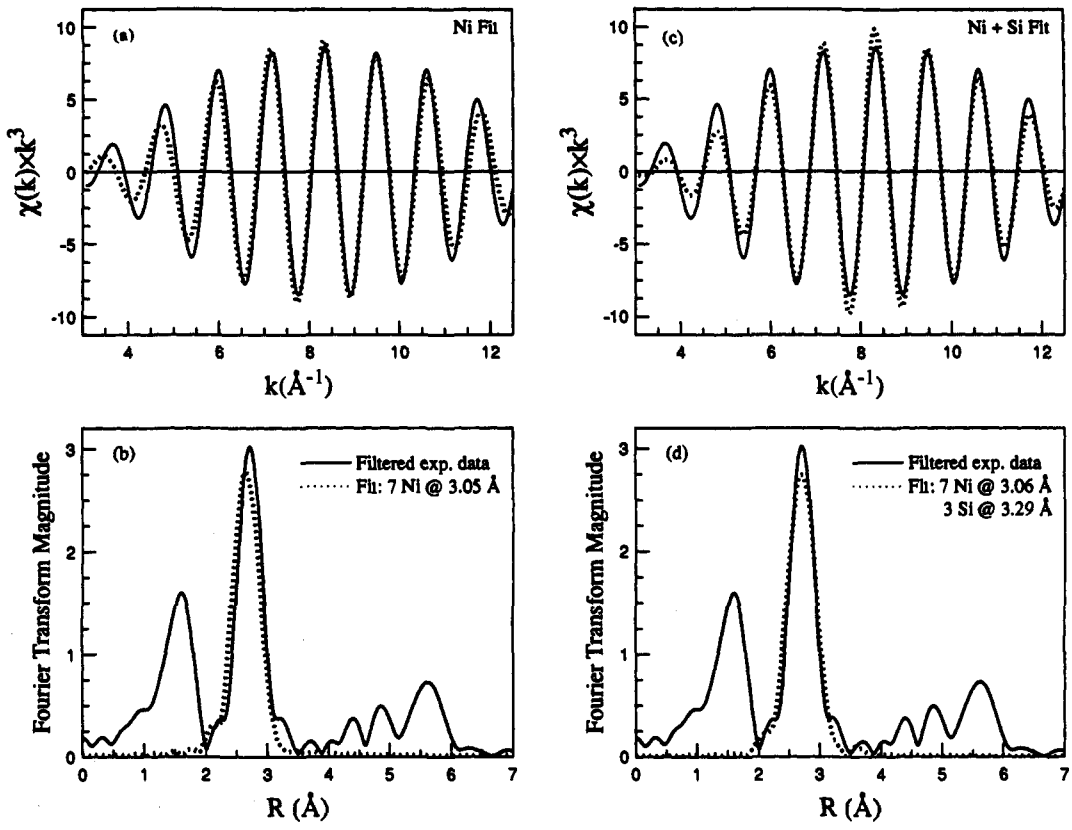

Figure 5. Filtered, experimental EXAFS spectrum (solid line) of the second RSF peak of nepouite and nonlinear least-squares fit (dots) using empirical phase-shift and amplitude functions for Co–Co from $Co(OH)_2$ and theoretical functions for Ni–Si from FEFF as references: (a) fit assuming one shell of Ni atoms with R, N, and σ^2 treated as adjustable parameters and ΔE_0 fixed; (b) RSFs (uncorrected for phase shift) of the experimental data and least-squares fit shown in a; (c) fit assuming one shell of Ni atoms and one shell of Si atoms with R and N treated as adjustable parameters and σ^2 and ΔE_0 fixed (Table 5) (four parameters varied); (d) RSFs (uncorrected for phase shift) of the experimental data and least-squares fit shown in c.

andradite, hedenbergite, and nepouite using Debye temperatures reported by Kieffer.[21] Because of a lack of data in the literature for natural compounds, our analysis was limited to these three compounds, and in the absence of data for hedenbergite and nepouite, we used Debye temperatures reported for compounds with similar structures and compositions (see Table 5). Comparison of the calculated σ^2 values to those derived from EXAFS fits and estimated from XRD rms displacements shows that the Debye model predicts values for σ^2 similar to those determined from the other methods only for Fe–Si in andradite and hedenbergite and much lower σ^2 values for all other absorber–backscatterer pairs. In these two compounds, Si is tightly bound in SiO_4 tetrahedra and has a low degree of static disorder. Thus, the Debye temperature probably more closely reflects the structure of the silicate sublattice. A simple Debye model cannot account for atomic static disorder that is inherent in many natural compounds, but may be useful in estimating σ^2 for tightly-bound atoms such as Si in complex compounds.

Multiple-Scattering. In most EXAFS models, it is assumed that single-scattering paths between the absorber and single shells of backscatterers have a much greater amplitude than MS paths in which the photoelectron wave "visits" more than one scattering atom. Photoelectron waves returning to the central atom from MS paths are thought to mostly cancel each other or undergo significant amplitude reductions because of inelastic scattering effects.[8] In some compounds, however, "forward-scattering" paths (also called focusing or shadowing) among linear or near-linear atoms have been shown to increase amplitude relative to single-scattering predictions.[22] Contributions to EXAFS from different types of MS paths are not usually examined in many compounds because of the lack of a usable (and convenient) theoretical model. The MS formulation in FEFF 5 greatly simplifies this analysis and was used to examine MS paths in all of the reference compounds (total R from 1 to 6.5 Å). In all compounds, the amplitudes predicted by FEFF 5 (with $\sigma^2 = 0$) for unfocused (i.e., nonlinear) MS paths were generally <10% of the amplitude predicted for the first-shell backscatterers. Most MS paths in these compounds involve nonlinear scattering through at least one oxygen atom, which was found to reduce scattering amplitudes severely compared to that among metal atoms.

In several compounds for which the FEFF model calculation predicted a significant (>10% of first-shell) amplitude to MS paths, filtered experimental data were fit to FEFF phase-shift and amplitude functions in order to estimate values for σ^2 for each path type.[23] The case for andradite is shown in Figure 6, in which two Fe → Si → O → Fe MS paths (total R = 3.52 and 3.67 Å) overlap with two single-scattering paths (Table 5) at similar distances over the R-range of the second RSF peak. We attempted to estimate σ^2 for these two MS paths by fitting the experimental data to the FEFF model with σ^2 adjusted and R, N, and ΔE_0 fixed for two single-scattering (Fe–Ca, Fe–Si) and two MS paths. In the least-squares fit, values of σ^2 for the MS paths were >0.02 Å² such that these paths contributed no amplitude to the EXAFS (Figure 6). Values of σ^2 determined by the Debye model for the MS paths were invariably too low (σ^2 = 0.0043–0.0056 Å²) and produced too much amplitude

(21) Kieffer, S. W. In *Microscopic to Macroscopic: Atomic Environments to Mineral Thermodynamics*, Kieffer, S. W., Navrotsky, A., Eds.; Mineralogical Society of America: Washington, DC, 1985; Vol. 14, pp 65–126.

(22) Teo, B.-K. *J. Am. Chem. Soc.* **1981**, *103*, 3990–4001. Boland, J. J.; Crane, S. E.; Baldeschwieler, J. D. *J. Chem. Phys.* **1982**, *77*, 142–153. Co, M.S.; Hendrickson, W. A.; Hodgson, K. O.; Doniach, S. *J. Am. Chem. Soc.* **1983**, *105*, 1144–1150. Bunker, G.; Stern, E. A. *Phys. Rev. Lett.* **1984**, *52*, 1990–1993.

(23) In the FEFF 5 multiple-scattering formulation, σ^2 represents mean-square displacements based on radial disorder of all atoms in a scattering path of total length R; see ref 7.

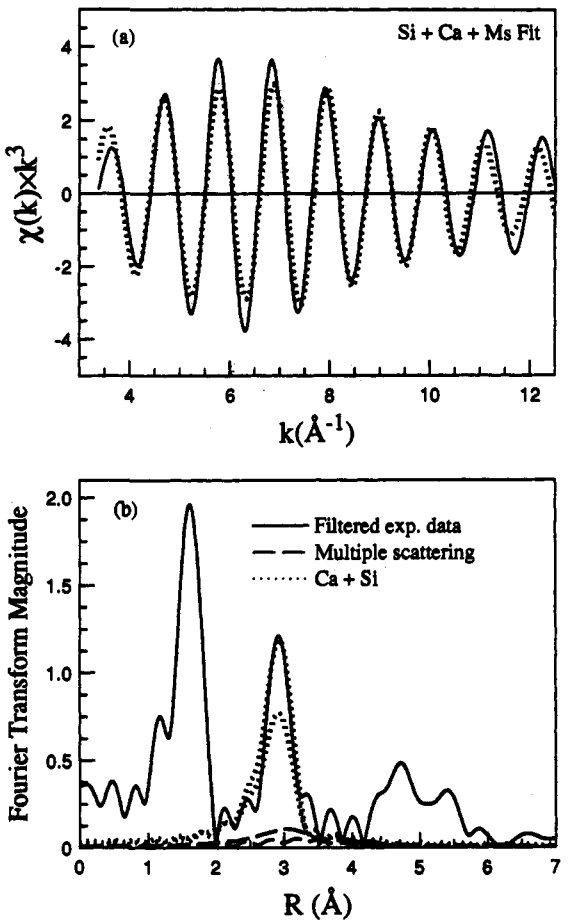

Figure 6. Filtered, experimental EXAFS spectrum (solid line) of the second RSF peak of andradite and nonlinear least-squares fit (dots) using FEFF theoretical phase-shift and amplitude functions as the reference. Two multiple-scattering (MS) paths predicted by FEFF to have significant amplitude are included in the model. (a) Fit assuming one shell of Si atoms at 3.37 Å, one shell of Ca atoms at 3.37 Å, and two shells of MS paths at 3.52 Å and 3.67 Å. R, N, and ΔE_0 were fixed for each shell; σ^2 for each shell was adjusted. (b) RSFs (uncorrected for phase shift) of experimental data and least-squares fit showing the relative contributions to amplitude from each of the four shells: dots = Ca (taller peak), Si (shorter peak); dashes = two MS paths.

compared with the experimental data. For all of the compounds of this study, Debye–Waller effects or destructive interferences effectively reduced EXAFS amplitude from unfocused MS paths below detection, probably because of the large number of oxygen atoms in these compounds. As expected, however, focused multiple-scattering (discussed next) was found to be significant in compounds with linear, equidistant atomic arrangements.

Focused Multiple-Scattering. Focused MS is significant in three of the reference compounds with layered crystal structures: $Co(OH)_2$, $Ni(OH)_2$, and $Ni_3Si_2O_5(OH)_4$ (nepouite). A peak in the RSFs of these three compounds at 5.2–6.4 Å results from linear single-scattering and MS among Me atoms at ≈3 and 6 Å (Figure 7a). The possible scattering paths can be analyzed by examining the atomic structures of these compounds in which the metal atoms are found in layers of closest-packed oxygen octahedra and oxygen atoms lie above and below planar Me atoms (Figure 7b). Surrounding each Me atom are six coplanar Me atoms at 3.07 Å (nepouite), 3.12 Å ($Ni(OH)_2$), or 3.17 Å ($Co(OH)_2$) and six more coplanar Me atoms at exactly twice that distance (6.14, 6.24, or 6.34 Å) (Figure 7c). There are other O and Me atoms at distances closer than 6 Å to the central absorber, but they are not coplanar with the 3- and 6-Å Me atoms. Because of the high symmetry, all distances between a central Me and Me atoms at 3 and 6 Å are the same, and thus, a large number of degenerate two-, three-, and four-leg scattering paths have a total distance of 6 Å without scattering among intervening oxygen atoms. Because these compounds are composed primarily of oxygen octahedra that apparently damp scattering, they lack large MS contributions from triangular paths that have been observed in metals with closest-packed structures.[7]

We calculated all single-scattering and MS paths in the structure of $Co(OH)_2$ with total $R = 6.346$ Å using FEFF 5 (with $\sigma^2 = 0$) to identify paths that may contribute significant amplitude to the EXAFS. Comparison of integrated path amplitudes indicates that all nonlinear paths are insignificant because of destructive interferences and that only three types of linear paths contribute significantly to the EXAFS (Figure 7c). If Co_1 is the absorber Co atom, Co_2 is a Co atom at 3.173 Å, and Co_3 is a Co atom at 6.346 Å, then paths of significant amplitude with total $R = 6.346$ Å are (Figure 7c) (1) "SS6", single-scattering to 6.346 Å, $Co_1 \rightarrow Co_3 \rightarrow Co_1$ (two legs, degeneracy = 6); (2) "MS6", MS involving scattering to Co_3 at 6.346 Å, either a three-leg path of $Co_1 \rightarrow Co_2 \rightarrow Co_3 \rightarrow Co_1$ or the inverse path, $Co_1 \rightarrow Co_3 \rightarrow Co_2 \rightarrow Co_1$, or four-leg paths, $Co_1 \rightarrow Co_2 \rightarrow Co_3 \rightarrow Co_2 \rightarrow Co_1$ (total degeneracy = 18); (3) "MS3", MS involving only Co_1 and Co_2 atoms on either side (Co_2 and $-Co_2$) at 3.173 Å, either $Co_1 \rightarrow Co_2 \rightarrow (-Co_2) \rightarrow Co_1$ (three legs), $Co_1 \rightarrow Co_2 \rightarrow Co_1 \rightarrow (-Co_2) \rightarrow Co_1$ (four legs), or $Co_1 \rightarrow Co_2 \rightarrow Co_1 \rightarrow Co_2$ (same atom twice, four legs; total degeneracy = 18). The theoretical phase-shift and amplitude functions predicted by FEFF are slightly different for each of these three path types, and accordingly, values for σ^2 are expected to differ among the different paths. Theoretical phase-shift and amplitude functions were compared to filtered experimental data for $Co(OH)_2$, R and N were fixed, and σ^2 was refined for each of the three path types described above ($\sigma^2 = 0.011$, 0.0094, and 0.0067, probably ±20–30%, for each path type, respectively). As shown in Figure 7d, the phase of the EXAFS oscillations is predicted quite well by the FEFF calculation. There is some mismatch in amplitude at high and low k between the experimental and theoretical EXAFS, perhaps because of overlap with other low-amplitude single-scattering paths. Comparison of the relative amplitudes of each path type shows that the focused MS paths have significantly greater amplitude than the single-scattering path and that linear focusing to atoms at 6.346 Å (MS6) produces more amplitude than scattering among atoms at 3.173 Å (MS3) (Figure 7d). This enhancement of scattering because of linear focusing has been used to analyze backscattering from atoms at distances much further from the central absorber than usually analyzed by single-scattering EXAFS to obtain longer range structural information.[6,24]

IV. Summary and Conclusions

Accurate determination of first- and higher-shell atomic coordination in complex crystalline solids containing mixtures of high- and low-Z atoms can be achieved with EXAFS analysis by using known reference compounds and *ab initio* calculations and by including effects from disorder and MS. Analysis of the EXAFS spectra of known compounds at ambient conditions shows that interatomic distances can be determined from single-scattering paths with high precision ($R < 0.02$ Å) to at least 4 Å from the central absorber using either empirical phase-shift and amplitude functions or theoretical functions generated by FEFF 5. The threshold energy parameter, ΔE_0, should be treated as an adjustable parameter in fitting the first coordination shell whether experimental or theoretical reference functions are used in order to obtain correct distances, but can be fixed in the analysis of atoms at greater R without introducing additional errors. Alternatively, ΔE_0 could be treated as a single adjustable parameter in a multiple-shell fit. If necessary, experimental

(24) O'Day, P. A.; Brown, G. E., Jr.; Parks, G. A. *J. Colloid Interface Sci.*, in press.

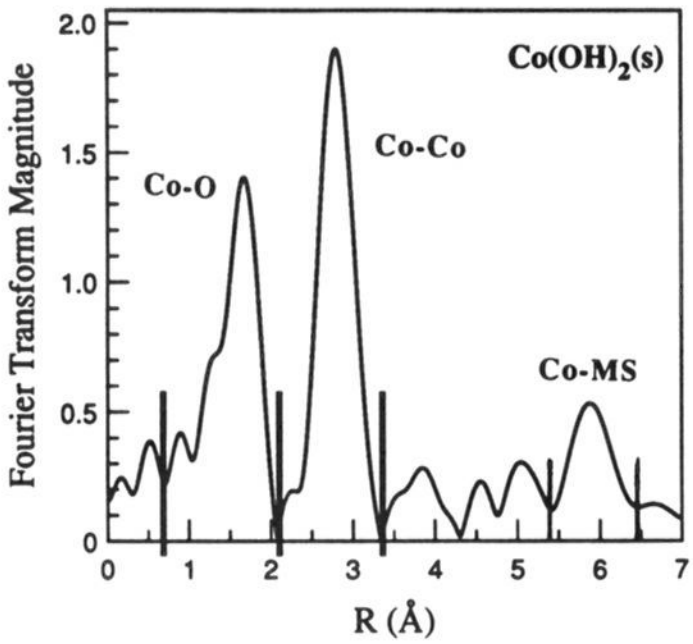

(a)

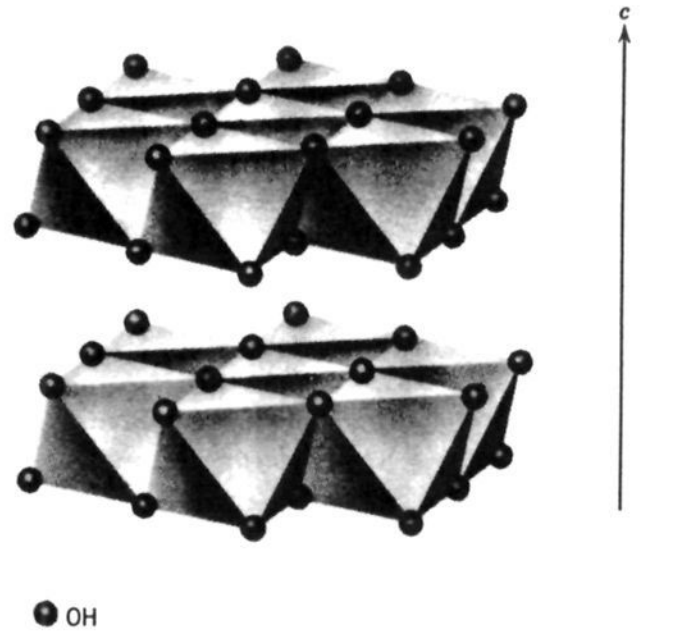

(b)

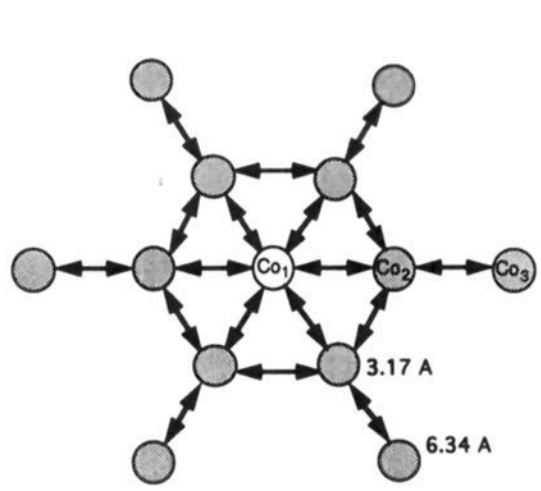

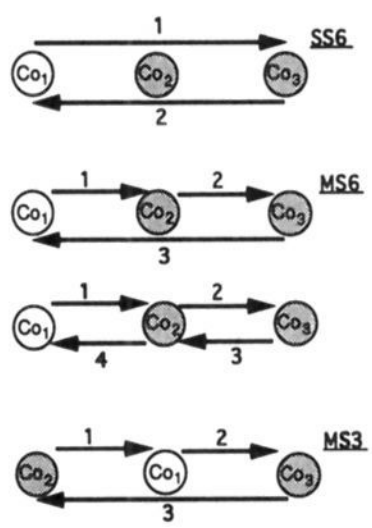

(c)

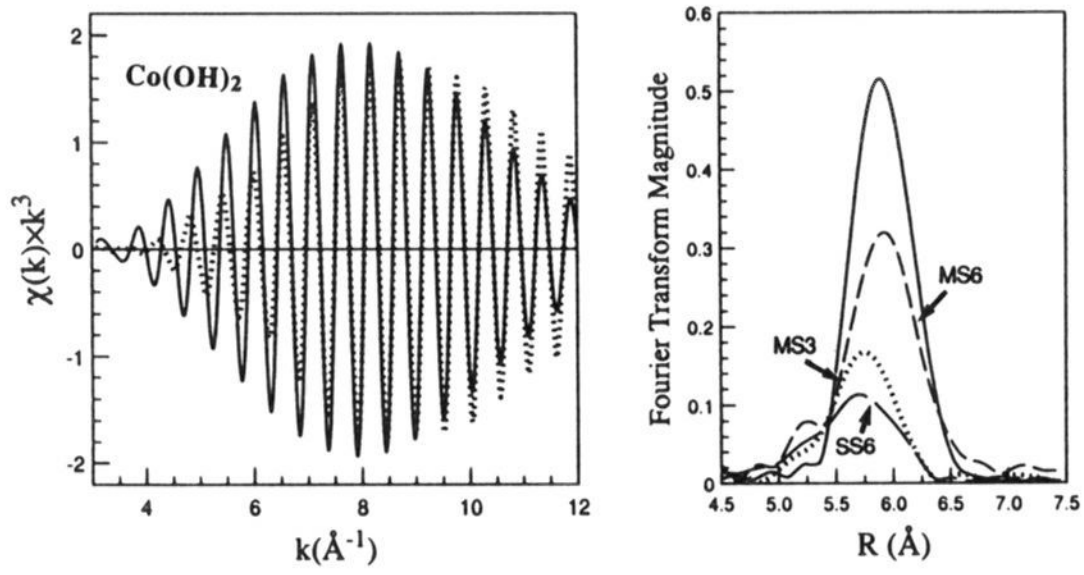

(d)

Figure 7. (a) RSF (uncorrected for phase shift) of $Co(OH)_2$. The peak at 5.5–6.4 Å is from focused multiple-scattering (MS). (b) Structure of $Co(OH)_2$ and $Ni(OH)_2$. The metal cation is six-coordinated by OH in layers of closest-packed, edge-shared octahedra. Layers are bonded perpendicular to the *c*-axis by hydrogen bonding. The Ni layer in nepouite has the same structure, but each octahedral layer is sandwiched between layers of Si tetrahedrally coordinated by O. (c) Coplanar arrangement of Co atoms in $Co(OH)_2$ with octahedral layers having equidistant, focused MS paths between a central absorbing atom (Co_1), Co atoms at 3.173 Å (Co_2), and Co atoms at 6.346 Å (Co_3) giving rise to three types of scattering paths, SS1, MS6, and MS3. (d) Theoretical FEFF EXAFS spectrum (dots) for single-scattering and focused MS paths in $Co(OH)_2$ a compared to the experimental filtered spectrum (solid line). The RSFs of the FEFF model is deconvoluted into relative contributions from SS6 (long dash), MS6 (dash), and MS3 (dots) paths and compared to the experimental RSF (solid line).

reference compounds for transition metals of central atom $Z \pm 1$ from the unknown can be used if the central atom has the same type of coordination environment in the reference and unknown structures. Use of the FEFF 5 theoretical code has several advantages over experimental standards; particularly important is (1) the ability to calculate reference functions for individual absorber–backscatterer pairs for atoms beyond the ligating shell where overlapping shells of atoms are typical in experimental compounds and (2) the elimination of errors introduced by differences in data collection and background subtraction among

experimental reference and unknown spectra. In EXAFS analysis of unknown compounds, combining analysis of experimental reference compounds, whose spectra inherently include disorder effects, with FEFF 5 calculations allows estimation of highly correlated parameters such as N, S_0^2, and σ^2, all of which contribute to EXAFS amplitudes. Determination of N to better than ± 1 can be achieved using FEFF 5 if experimental reference compounds are used to estimate values of S_0^2 and σ^2 for similar types of compounds.

At distances beyond the first coordination shell, backscattering, in the absence of shadowing, is dominated by metal–metal single-scattering in the compounds of this study. Elements of low Z can be analyzed for R and N if there are no other strong backscatterers at similar distances. In favorable cases, the number of backscatterers of different Z at similar distances can be determined to within about ± 1 if highly correlated parameters such as S_0^2 and σ^2 can be constrained. Values of σ^2 (about ± 20–30%) for individual scattering paths can be estimated using (1) analysis of known reference compounds with similar absorber–backscatterer coordination, (2) estimates from XRD rms displacements, or (3) a correlated Debye model for tightly-bonded atoms with relatively low disorder. Large atomic static disorder in some compounds is probably responsible for significant reductions in backscattering amplitudes. Temperature-dependent EXAFS studies, however, would be useful in constraining thermal contributions to σ^2. In unknown systems, it may be difficult to predict when static disorder will be large without prior knowledge of the structure or independent information from other techniques.

We find that MS paths that may contribute to EXAFS are reliably predicted with FEFF 5, and path-dependent, composite σ^2 values can be estimated from comparison of experimental and theoretical spectra. Other EXAFS analysis packages in general use can also treat MS. For example, the program EXCURV calculates MS paths with up to three scatterers using the rapid exact formalism of Binstead *et al.*[25] and, unlike FEFF 5, also contains data analysis capabilities. The FEFF 5 code calculates MS terms based on the Rehr–Albers MS approximation,[10] which is nearly exact but much faster. In addition, path discrimination implemented in FEFF 5 greatly facilitates calculation and examination of a large number of scattering paths in a given cluster and is not restricted to triple-scattering paths. FEFF 5 also uses an automated phase-shift calculator which does not require user input of muffin-tin radii or constant imaginary potentials.

In the compounds examined in this study, contributions to EXAFS from MS are generally not significant if scattering is nonlinear or among at least one low-Z atom (e.g., oxygen). This is in contrast to MS in metals, where nonlinear MS can be important.[7] The dominant type of MS in the reference compounds of this study is metal–metal focused scattering in the absence of intervening oxygen atoms. Other studies[6,22] have shown that linear focusing is common and may contribute significant amplitude to EXAFS even among low-Z atoms, suggesting that focused MS, if suspected, should be examined routinely in different cases. Given favorable geometric conditions, focused scattering permits analysis of atoms well beyond the R-range (>6 Å) typically accessible by single-scattering EXAFS, even at ambient temperatures.

Acknowledgment. Thanks to C. Chisholm-Brause, F. Farges, B. Hedman, W. Jackson, and G. Waychunas for assistance with data collection, analysis, and interpretations, and to M. Newville and E. Stern for helpful discussions. Some of the samples used in this study were kindly provided by C. Caly, B. Hedman, and A. Manceau. We thank G. Waychunas, S. Towle, and two anonymous reviewers for helpful comments and suggestions on the manuscript. Financial support was provided by the National Science Foundation through Grants EAR-8805440 and EAR-9105015 (G.E.B.) and by the Department of Energy through Grant DE-FG06-ER45415-A003 (J.J.R. and S.I.Z.). Work was done (partially) at SSRL, which is operated by the Department of Energy, Office of Basic Energy Sciences. The SSRL Biotechnology Program is supported by the NIH, Division of Research Resources, and DOE, Office of Health and Environmental Research.

(25) Gurman, S. J.; Binstead, N.; Ross, I. *J. Phys. C: Solid State Phys.* **1984**, *17*, 143–151. Gurman, S. J.; Binstead, N.; Ross, I. *J. Phys. C: Solid State Phys.* **1986**, *19*, 1845–1861.